



Cite this: *Food Funct.*, 2024, **15**, 4936

Dietary supplementation with *Lacticaseibacillus rhamnosus* IDCC3201 alleviates sarcopenia by modulating the gut microbiota and metabolites in dexamethasone-induced models†

Minkyung Kang,^a Minji Kang,^a Jiseon Yoo,^a Juyeon Lee,^a Sujeong Lee,^a Bohyun Yun,^b Minhong Song,^c Jun-Mo Kim,^d Hyung Wook Kim,^e Jungwoo Yang,^f Younghoon Kim ^{*g} and Sangnam Oh ^{*a}

Probiotics can exert direct or indirect influences on various aspects of health claims by altering the composition of the gut microbiome and producing bioactive metabolites. The aim of this study was to examine the effect of *Lacticaseibacillus rhamnosus* IDCC3201 on skeletal muscle atrophy in dexamethasone-induced C2C12 cells and a mouse animal model. Dexamethasone treatment significantly reduced C2C12 muscle cell viability, myotube diameter, and levels of muscle atrophic markers (Atrogin-1 and MuRF-1). These effects were alleviated by conditioned media (CM) and cell extract (EX) derived from *L. rhamnosus* IDCC3201. In addition, we assessed the *in vivo* therapeutic effect of *L. rhamnosus* IDCC3201 in a mouse model of dexamethasone (DEX)-induced muscle atrophy. Supplementation with IDCC3201 resulted in significant enhancements in body composition, particularly in lean mass, muscle strength, and myofibril size, in DEX-induced muscle atrophy mice. In comparison to the DEX-treatment group, the normal and DEX + *L. rhamnosus* IDCC3201 groups showed a higher transcriptional level of myosin heavy chain family genes (MHC1, MHC1b, MHC2A, 2bB, and 2X) and a reduction in atrophic muscle makers. These analyses revealed that *L. rhamnosus* IDCC3201 supplementation led to increased production of branched-chain amino acids (BCAAs) and improved the *Allobaculum* genus within the gut microbiota of muscle atrophy-induced groups. Taken together, our findings suggest that *L. rhamnosus* IDCC3201 represents a promising dietary supplement with the potential to alleviate sarcopenia by modulating the gut microbiome and metabolites.

Received 13th December 2023,
Accepted 23rd March 2024

DOI: 10.1039/d3fo05420a

rsc.li/food-function

1. Introduction

Muscle is an essential tissue that accounts for the most plentiful and prominent portion of total body protein in humans and regulates the balance between protein breakdown and

synthesis.^{1,2} In addition, muscles can affect inflammation, energy/nutrient metabolism, insulin resistance, and oxidative stress.² The process of aging contributes to increased muscle protein breakdown, primarily as a result of inflammation and oxidative stress, leading to conditions such as muscle atrophy (sarcopenia) or cachexia.^{3–6} These conditions have a detrimental impact on the overall quality of health, increasing the risk of fractures, physical limitations, and mortality.⁵ Consequently, the preservation of healthy muscle mass and the prevention of muscle atrophy are of paramount importance in the prevention of a range of diseases and the promotion of health claims.^{2,7}

Probiotics are live microbiota that provide health benefits to the host by maintaining the homeostasis of the intestinal microbiota and the immune system and possessing anti-inflammatory and anti-aging properties in human and animal.^{8–18} Recent studies have shown that *Lacticaseibacillus rhamnosus* species are probiotics, a type of intestinal bacteria, and have been reported to provide various biological activi-

^aDepartment of Food and Nutrition, Jeonju University, Jeonju 55069, Republic of Korea^bHonam National Institute of Biological Resources, Mokpo 58762, Republic of Korea.^cDepartment of Animal Science and Biotechnology, Chungnam National University, Daejeon 34134, Republic of Korea^dDepartment of Animal Science and Technology, Chung-Ang University, Anseong 17546, Gyeonggi-do, Republic of Korea^eCollege of Life Sciences, Sejong University, Seoul 05006, Republic of Korea^fDepartment of Microbiology, College of Medicine, Dongguk University, Gyeongju, 38066, Republic of Korea^gDepartment of Agricultural Biotechnology and Research Institute of Agriculture and Life Science, Seoul National University, Seoul 08826, Republic of Korea†Electronic supplementary information (ESI) available. See DOI: <https://doi.org/10.1039/d3fo05420a>

ties:¹⁹ anti-inflammatory,²⁰ anti-obesity,²¹ immune modulation,²² gut health (IBD and IBS),^{23–25} and cholesterol level reduction. In addition, the *Lactocaseibacillus rhamnosus* IDCC3201 strain used in our study was isolated from infant feces, and it has been confirmed to be¹⁸ anti-allergic,²⁶ anti-inflammatory, anti-pathogenic,¹⁹ and immunomodulatory.²⁷ However, the beneficial effect of *L. rhamnosus* on sarcopenia by regulating gut microbial balance is yet unknown.

Recent research has introduced the novel concept of the 'gut-muscle axis', highlighting the potential direct and indirect impacts of gut microbiome composition and metabolites on skeletal muscle function.^{28–32} Probiotic bacteria can alter the gut microbiome composition and modify the metabolic output, such as short-chain fatty acids (SCFAs), during the gut fermentation process.^{3,6,33,34} SCFAs, including propionate, butyrate, and acetate, affect muscle strengthening by regulating several aspects, including skeletal muscle mass, function, and metabolism.³⁵ Additionally, branched-chain amino acid (BCAA) supplementation alleviates muscle atrophy in angiotensin II-induced atrophy mice, which attenuates the reduction in exercise capacity.³⁶ Hence, this evidence suggests the significance of probiotics in modulating the gut environment and generating these bioactive metabolites as a critical factor in the prevention of sarcopenia.

In this study, we hypothesized that the administration of *L. rhamnosus* IDCC301 probiotics could offer potential benefits in addressing sarcopenia through the modulation of gut microbiome composition and the production of bioactive metabolites. To investigate this hypothesis, we comprehensively investigated the effects of *L. rhamnosus* IDCC3201 using C2C12 murine myoblasts and a sarcopenia mouse model induced by dexamethasone (DEX).

2. Materials and methods

2.1 *Lactocaseibacillus rhamnosus* IDCC3201 culture and preparation

Lactocaseibacillus rhamnosus IDCC3201 was inoculated in Man Rogosa Sharpe broth (MRS; BD, USA) and then cultured at 37 °C for 48 h. For *in vitro* experiments, the CM of IDCC3201 was prepared as described previously.³⁷ Briefly, *L. rhamnosus* IDCC3201 was grown in MRS broth at 37 °C for 48 h, harvested by centrifugation, and washed twice with 1× phosphate-buffered saline (PBS). Following centrifugation, the IDCC3201 pellet was incubated in DMEM cell culture media and cultured overnight at 37 °C. IDCC3201-CM was produced by centrifuging cultured DMEM to remove bacteria and filtering with a sterile filter with a 0.2 µm pore size. Next, IDCC3201-CM was adjusted to pH 7.0 using 5 N NaOH.

The cell extract (EX) was prepared as described by Lin *et al.*⁴⁴ with some modifications. Briefly, a pellet of IDCC3201 was cultured in MRS broth and resuspended in a minimal volume of 1× PBS and then ultrasonicated using an ultrasonic homogenizer (KUS1200, KBT, Seongnam, Korea) to lyse the bacterial cell walls on ice (condition; for 3 min with 0.5 s inter-

vals at 60 W, for a total of 60 cycles). The protein concentration of EX was determined using the Bradford assay supplied by Bio-Rad (Hercules, CA, USA) and compared with multiple concentrations of BSA. For *in vivo* studies, the IDCC3201 culture was collected by centrifugation at 3500 rpm for 10 min at room temperature. The pellet of IDCC3201 was resuspended in saline to achieve a final concentration of 10⁹ colony-forming units per milliliter (CFU per mL). The prepared solution was used on the day of preparation and subsequently stored at –20 °C for further use.

2.2 C2C12 cell culture and differentiation

Undifferentiated myoblast C2C12 cell lines were maintained in DMEM supplemented with 10% heat-inactivated FBS (Welgene, S101-01) and 1% anti-anti (Gibco, 15240062) in a 5% CO₂ humidified atmosphere at 37 °C. Differentiation was induced by supplementation with heat-inactivated 2% horse serum (Sigma, H1138) instead of 10% FBS to differentiate myoblast cells into myocytes. When myoblasts were approximately 80% confluent, the growth medium (GM) was replaced with differentiation medium (DM) once every two days for six days. Next, differentiated myotubes were treated in serum-free media (SFM) containing various concentrations of cell extract (EX; 0.01, 0.1, and 10 µg mL^{–1}) or conditioned medium (CM; 0.01, 0.1, 1, and 2% of cell working volume) for 24 h. Dexamethasone (DEX; 100 µM) was used to induce myotube cell atrophy.

2.3 Cell viability and cytotoxicity assay

To assess cell viability, C2C12 myoblast cells (1 × 10⁴ cells per cm²) were seeded into 48-well plates using growth medium and incubated at 37 °C for 24 h to allow attachment. The attached cells were treated with or without CM or EX for 24 h. For the cytotoxicity assessment, following the same seeding and incubation process, the C2C12 myoblast cells were differentiated into myocyte cells. Once attached, these cells were treated with DEX in combination with either CM or EX for 24 h. The MTT assay was subsequently employed for both viability and cytotoxicity evaluations. An MTT solution (100 µl) was introduced to each sample, followed by incubation at 37 °C for 2 h. Then, 0.5 ml of DMSO was dispensed into each well, and further incubation was carried out for 30 min at room temperature. Absorbance values were transferred to a 96-well plate and quantified using a microtiter plate reader (Synergy HT, BioTek Instruments, Winooski, VT) at a wavelength of 570 nm.

2.4 PAS staining and measurement of myotube diameters

Myotube cells were subjected to periodic acid-Schiff (PAS) staining using a kit procured from VitroVivo Biotech (Rockville, MD) according to the manufacturer's instructions. Briefly, the cells were first rinsed with cold 1× PBS and then fixed for 5 min using 4% paraformaldehyde. A gentle washing step using 1× PBS was then carried out, after which the cells were incubated with 1% periodic acid for a span of 10 min. Then, two 5-minute washes with distilled water were per-



formed. The samples were then exposed to Schiff's reagent for 40 min, followed by three wash steps every 5 min with distilled water. The nuclei were counterstained using Meyer's hematoxylin for a duration of 1 min, which was followed by three washes, each 5 min with distilled water. Images were randomly selected using a microscope fitted to a digital camera, and the myotube diameter size was determined using ImageJ software.

2.5 Giemsa staining and fusion index scoring

After differentiation, the cells were rinsed twice with 1× PBS and subsequently fixed using 4% paraformaldehyde for 10 min. Following fixation, the cells were incubated with a 1:20 diluted Giemsa stain modified solution (32884, Sigma) in 1 mM sodium phosphate buffer (pH 5.6), amounting to 1 ml, for a duration of 40 min. Imaging of the cells was evaluated by a microscope equipped with a digital camera. Quantitative assessment involved measuring both the total cell nuclei and the proportion of nuclei residing within the myotubes, ensuring that at least 100 nuclei were evaluated per well. The fusion index score was derived by dividing the number of nuclei identified within myotubes by the overall number of counted nuclei.

2.6 Myosin heavy chain (MHC) immunofluorescence assay

C2C12 myotubes were washed with 1× PBS once, followed by fixation using 4% paraformaldehyde for a period of 20 min. Then, they were washed twice with 1× PBS. For permeabilization, the cells were treated with 0.2% Triton X 100 in 1× PBS for 5 min. Postpermeabilization, a blocking step was instituted using 1% bovine serum albumin (BSA) and maintained for 45 min at room temperature. The myotubes were then incubated with an MHC primary antibody (1:250 dilution, Santa Cruz, TX, USA) at 4 °C overnight. Following three washes with 0.1% PBST, these cells were exposed to a secondary antibody conjugated with Alexa Fluor 488 (1:1000 dilution, Invitrogen, MA, USA) for 1 h at room temperature in a dark room. After washing twice with 0.1% PBST, nuclear staining was executed using prolonged gold antifade mountant integrated with DAPI (P36931, Invitrogen). Imaging of the C2C12 myotube cells was conducted using a fluorescence microscope. For MHC-positive area analysis, six randomly selected regions were assessed from three wells per group. Both the fusion index score and MHC-stained region were quantified and evaluated utilizing ImageJ software. The fusion index of myotubes was determined by calculating the ratio of nuclei present within the myotubes to the total number of nuclei observed.³⁸

2.7 Quantitative real-time PCR (qRT-PCR) assay

Total RNA from C2C12 myocyte cells and mouse quadriceps femoris muscle was extracted. C2C12 cells were harvested with 1 ml of QIAzol lysis reagent. Mouse quadriceps femoris muscle (QD, 0.1 g) was mixed with QIAzol lysis reagent and homogenized using a taco™ Prep Bead Beater for 13 s in two cycles. According to the manufacturer's protocol, RNA was extracted using a Monarch Total RNA Miniprep Kit (New England Biolabs, MA, USA). After RNA was extracted, cDNA was syn-

thesized by a cDNA synthesis kit (iScript cDNA synthesis kit, Bio-Rad). Real-time qPCR was performed using Luna Universal qPCR Master Mix (NEB) in a Step One Plus real-time PCR system (Applied Biosystems, Carlsbad, CA, USA) to measure the mRNA levels of muscle atrophic factors (Atrogin-1, MuRF-1, and myostatin), myosin heavy chains (MHC1, MHC2A, MHC2B, and MHC2X), and inflammatory cytokines (IL-6). An internal control was established using mRNA for β -actin. The reaction conditions were as follows: pre-cycling at 95 °C for 1 min, followed by 35 cycles of 90 °C for 30 s and 60 °C for 30 s and melting at 95 °C for 15 s and 60 °C for 1 min. All the results were normalized to the housekeeping gene β -actin. The relative mRNA expression level was calculated with the $2^{-\Delta\Delta C_t}$ method.

2.8 Western blotting assay for protein expression

Postexposure to either EX or CM, C2C12 myocyte cells were harvested and lysed using RIPA buffer formulation (containing 50 mM Tris-HCl, 150 mM NaCl, 1.0% (v/v) NP-40, 0.5% (w/v) sodium deoxycholate, 1.0 mM EDTA, 0.1% (w/v) SDS, and 0.01% (w/v) sodium azide with a pH adjusted to 7.4) with a 100× concentration of protease and phosphatase inhibitor cocktail for 30 min at 4 °C. Then, the proteins were separated by 12% SDS-PAGE and transferred to PVDF membranes at a constant current of 200 mA for 4 h. The PVDF membranes were then blocked using 5% skim milk in TBST buffer. After blocking, the membranes were incubated overnight at 4 °C with primary antibodies specific to Atrogin-1, MuRF-1, and B-actin (from Santa Cruz), with dilution ratios of either 1:250 or 1:1000 (specifically for B-actin). After primary antibody incubation, the membranes were washed with TBST buffer and then incubated with secondary antibodies at a dilution of 1:5000 for 1 h at room temperature. Protein bands were then visualized and quantified based on their intensities using the Azure 300 Gel Imaging System (Azure Biosystems, CA).

2.9 Animals and experimental procedure

The experiment was approved by the Institutional Animal Care and Use Committee of The Food Industry Promotion Agency of Korea, Iksan, Korea (IACUC-22-016). Six-week-old male C57BL/6J mice were purchased from Orient Bio (Seongnam, Korea) and housed under a 12 h light/dark cycle with $55 \pm 5\%$ relative humidity and a temperature of 23 ± 1 °C. After a week of acclimatization, the mice were given either saline or IDCC3201 (1×10^8 CFU per 100 μ l saline) daily. At the age of seven weeks, the mice were randomly divided into three groups: the normal group received intraperitoneal saline injections, the DEX group was treated with dexamethasone in 9% Kolliphor® HS 15 (42966, Sigma-Aldrich, MO, USA) + 10% DMSO starting from the fourth week for nine days, and the DEX + IDCC3201 group had the same DEX treatment with an addition of 10^8 CFU per 0.1 ml IDCC3201. On day 35, the muscle strength of the mice was assessed using a hand grip test, which was conducted five times for each subject. Lean body mass measurements were taken *via* nuclear magnetic resonance on days 14, 28, and 36. After the evaluations, the



mice were euthanized, and three types of skeletal muscle tissues (quadriceps, gastrocnemius, and tibialis anterior) were collected, weighed, and stored at -80°C until further analysis.

2.10 Histology

Muscle fiber atrophy was examined histologically through hematoxylin and eosin (H&E) staining. The muscle tissue was fixed in 4% paraformaldehyde. The cross-sectional area (CSA) of the myofibrils was quantified using ImageJ software, with a minimum of 100 fibers per sample counted at $200\times$ magnification.

2.11 Fecal metagenomic analysis

Fresh fecal samples were collected from each mouse at six weeks after the induction of muscle atrophy. For the extraction of bacterial genomic DNA, fecal samples were resuspended in QIAzol and homogenized using a tacoPrep Bead beater for two cycles, each lasting 13 s. Following homogenization, samples were centrifuged at $15\,000g$ for 15 min. Genomic DNA was then extracted using the PowerSoil Pro kit from Qiagen as per the manufacturer's instructions. The subsequent analysis of microbial diversity and metagenomic profiles was conducted as previously described.³⁹ The V4 region of the 16S rRNA gene was amplified and sequenced using the MiSeq system by Illumina at Macrogen. Data processing was carried out with Mothur, following the standard protocol.⁴⁰ Alpha diversity, such as Chao1, Shannon, and Simpson, along with the relative abundance at the phylum, family, and genus levels, were analyzed using the MicrobiomeAnalyst web-based platform.⁴¹

2.12 Fecal metabolome analysis

For fecal metabolome analysis, fresh feces were collected and suspended in methanol at a 20 mg mL^{-1} concentration. After vortexing for 5 min on ice, the samples were centrifuged ($15\,000g$, 5 min, 4°C), and the supernatant was filtered through $0.2\text{ }\mu\text{m}$ syringe filters (Whatman, England). The filtered supernatant was then subjected to trimethylsilyl derivatization by adding $50\text{ }\mu\text{L}$ of *N,O*-bis(trimethylsilyl)trifluoroacetamide (BSTFA; Sigma) containing 1% trimethylchlorosilane (TMCS) and $30\text{ }\mu\text{L}$ methoxyamine hydrochloride in pyridine (20 mg mL^{-1}). This mixture was incubated for 90 min at 30°C . The derivatized samples were analyzed using a Thermo Trace 1310 GC coupled with a Thermo ISQ LT mass spectrometer. Utilizing a DB-5 MS GC column (Agilent), helium was employed as a carrier gas at a flow rate of 7.5 mL min^{-1} . The temperature settings were 300°C for injection and a staged oven ramp temperature starting from 50°C . Spectral analysis was conducted using AMDIS software, and metabolites were identified against the NIST Mass Spectral Search program (version 2.0, Gaithersburg, MD, USA). Finally, metabolite data normalization was performed based on the intensity of the internal fluoranthene standard.

2.13 Statistical analysis

Statistical analyses were conducted using GraphPad Prism (version 9.5.0). Group differences were assessed through a one-

way analysis of variance (ANOVA) followed by Tukey's *post hoc* tests. For direct comparisons, unpaired *t* tests were employed. All data were independently replicated in triplicate. *P* values < 0.05 were considered statistically significant. Comparisons of microbiome alpha diversity (Chao1, Shannon, and Simpson indices) and the abundance of fecal bacteria were executed by unpaired *t* tests. Heatmaps and one-way ANOVA modules were used in the MetaboAnalyst 5.0 web-based platform to identify metabolite changes.

3. Results

3.1 *L. rhamnosus* IDCC3201 mitigates dexamethasone-induced C2C12 myotube atrophy

The gut microbiota plays a crucial role in orchestrating the functions of other organs generating energy and metabolites⁴² within the gastrointestinal tract and facilitating their transport across the intestinal barrier.^{35,43} As a potential probiotic bacterium, we expected that *L. rhamnosus* IDCC320 would indirectly affect muscle by generating metabolites through its positive role in the gastrointestinal tract. Conditioned medium (CM) and ultrasonication techniques are crucial in obtaining valuable metabolites from bacteria, and their efficiency in producing cell extracts (EX) enriched in bioactive compounds and enzymes has been demonstrated.^{44,45} Several studies suggested that the CM method or EX (extracted by ultrasonication) contains numerous chemical compounds and beneficial proteins or factors released by bacteria with similar effects to live bacteria.^{37,46} Thus, we prepared cell extract (EX) samples containing cellular components such as peptidoglycans and surface proteins or crude cell extracts derived from *L. rhamnosus* IDCC3201. In addition, we prepared conditioned medium (CM) as a postbiotic supplement containing metabolites secreted by probiotics.⁴⁷ The primary objective of this study was to assess the impact of *L. rhamnosus* IDCC3201 on muscle atrophy in C2C12 murine muscle cells. To determine the optimal concentration range of *L. rhamnosus* IDCC3201-CM or EX, the MTT assay was performed to evaluate the cell viability of myoblasts and atrophy-induced myotubes. In both myocytes and myotubes, no cytotoxic effect was observed by *L. rhamnosus* IDCC3201-CM or EX treatment at all concentrations for 24 h (Fig. 1A–D). Therefore, 1.0 and $10.0\text{ }\mu\text{g mL}^{-1}$ from the EX sample and 1% and 2% from the CM sample were selected and applied in subsequent experiments.

The protective effects of *L. rhamnosus* IDCC3201 CM or EX against muscle atrophy in C2C12 myotubes triggered by DEX were evaluated through the measurement of the myotube diameter using PAS and Giemsa staining assays. Treatment with DEX notably diminished the myotube diameter when contrasted with the control (without DEX). Conversely, both DEX + CM (1 and $10\text{ }\mu\text{g mL}^{-1}$) and DEX + EX (1 and 2%) treatments led to a significant enhancement in the myotube diameters relative to the DEX group (Fig. 1E and F): PAS staining (control, $31.60 \pm 1.44\text{ }\mu\text{m}$; DEX, $22.84 \pm 1.65\text{ }\mu\text{m}$; DEX + CM 1 and $10\text{ }\mu\text{g mL}^{-1}$, $25.66 \pm 1.48\text{ }\mu\text{m}$, and $24.42 \pm 0.89\text{ }\mu\text{m}$; DEX +



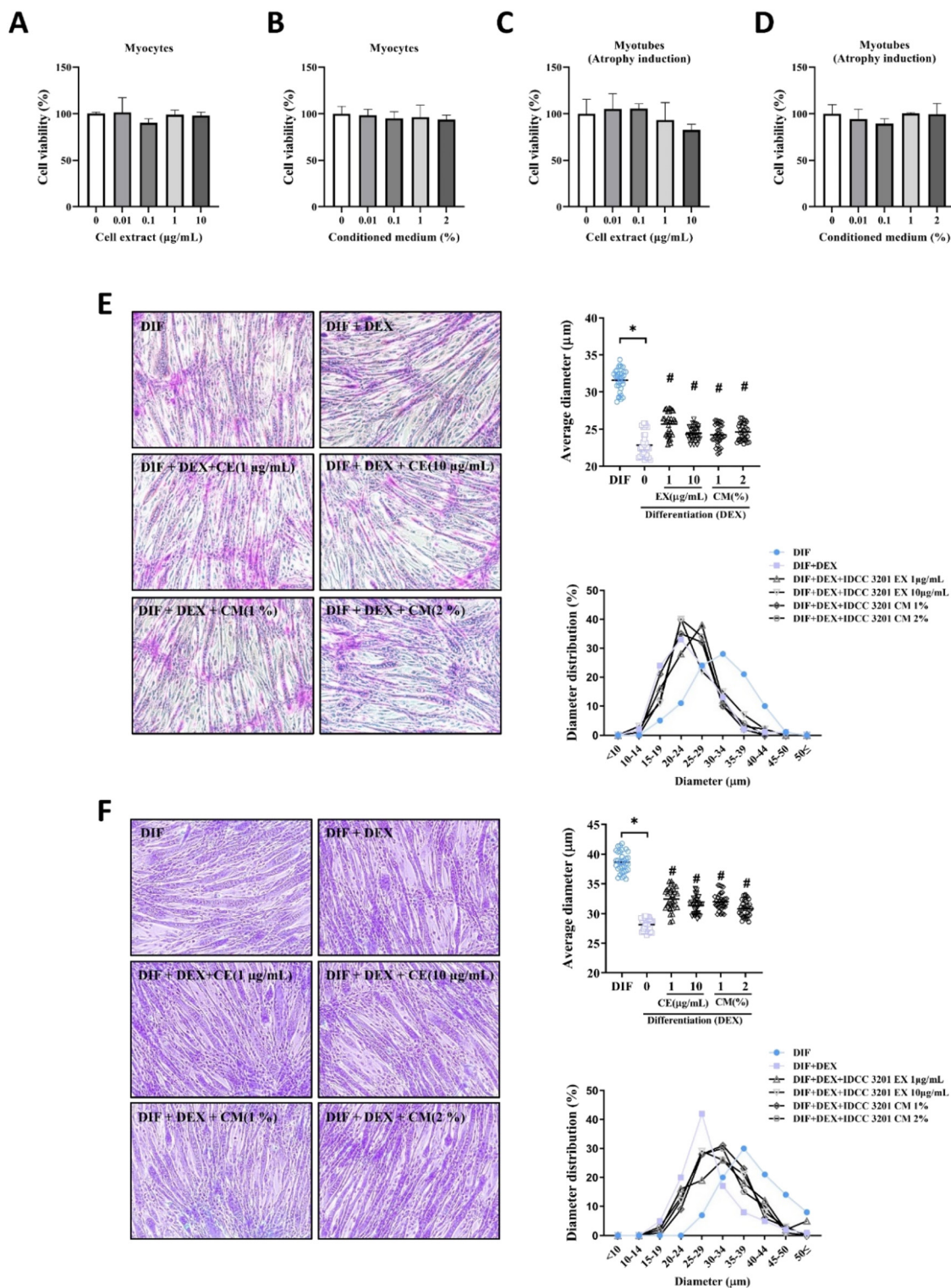


Fig. 1 *L. rhamnosus* IDCC3201 inhibits DEX-induced muscle atrophy in C2C12 cells. (A and B) Cell viability assays displaying the impact of various treatments on C2C12 myoblast or (C and D) myotube cells. (E) Representative images from PAS staining of myotubes subjected to DEX treatment in conjunction with varying concentrations of IDCC3201 CM or EX. (F) Giemsa-stained images highlighting the morphological changes in myotubes following treatment. Statistical significance was determined by an unpaired t test. * $P < 0.05$ vs. DIF. # $P < 0.05$ vs. DIF + DEX.

EX 1 and 2%, $24.24 \pm 1.27 \mu\text{m}$, and $24.61 \pm 1.12 \mu\text{m}$), Giemsa staining (control, $38.63 \pm 1.67 \mu\text{m}$; DEX, $28.13 \pm 1.01 \mu\text{m}$; DEX + CM 1 and $10 \mu\text{g mL}^{-1}$, $32.47 \pm 1.76 \mu\text{m}$, and $31.34 \pm 1.35 \mu\text{m}$;

DEX + EX 1 and 2%, $32.01 \pm 1.36 \mu\text{m}$, and $30.8 \pm 1.32 \mu\text{m}$). After treatment with *L. rhamnosus* IDCC3201-CM and EX, the diameter distribution recovered to the level of the control



group. Immunofluorescence analysis of myosin heavy chain (MHC) expression demonstrated the critical impact of *L. rhamnosus* IDCC3201 in mitigating myotube atrophy induced by DEX. Notably, even though the DEX group exhibited a significant reduction in MHC expression in myotubes, the presence of *L. rhamnosus* IDCC3201 significantly exhibited a positive effect in preserving MHC levels under these atrophy-inducing conditions (Fig. 2A). Similar results were also observed in the fusion index (Fig. 2B). These results indicate that *L. rhamnosus* IDCC3201 and its metabolites markedly prevent DEX-induced myotube atrophy in C2C12 myotubes cells.

3.2 *L. rhamnosus* IDCC3201 reduced the expression of muscle atrophic markers in C2C12 myotubes

The ubiquitin–proteasome system (UPS) specifically induces the degradation of muscle proteins,⁴⁸ and Atrogin-1 and MuRF-1 play essential roles as E3 ubiquitin ligases in the UPS.⁴⁹ Accordingly, we measured the mRNA levels of atrophic muscle markers (Atrogin-1 and MuRF-1) in C2C12 myotube cells. The DEX group showed a significant increase in the expression levels of Atrogin-1 and MuRF-1 and a decrease in the expression levels of MyoD (muscle differentiation factor) compared to the control group. In contrast, 10 $\mu\text{g mL}^{-1}$ IDCC3201-EX significantly reduced Atrogin-1 and MuRF-1 in C2C12 myotube cells treated with DEX (Fig. 3A and B). However, IDCC3201-CM treatment only reasonably reduced the protein levels of Atrogin-1 and MuRF-1 (Fig. 3D and E). CM and EX significantly increased MyoD levels in common compared to the DEX group (Fig. 3C). While neither the conditioned medium (CM) nor the cell extract (EX) displayed a significant inhibition of Atrogin-1 and MuRF-1 expression, our *in vitro* findings suggest that they clearly exhibit an anti-atrophic effect. To demonstrate these *in vitro* results, we next

assessed the effect of *L. rhamnosus* IDCC3201 in a sarcopenia-induced *in vivo* mouse model.

3.3 *L. rhamnosus* IDCC3201 increases muscle fiber size and enhances muscle strength in the C57BL/6 sarcopenia mouse model

To evaluate the effects of *L. rhamnosus* IDCC3201 on muscle atrophy, we assessed the DEX-induced sarcopenia mouse model and investigated muscle function *in vivo*. Considering the preventive effects of *L. rhamnosus* IDCC3201 as a probiotic on sarcopenia, mice were pretreated with 10^8 CFU per 100 μL of *L. rhamnosus* IDCC3201 in saline by oral gavage for 4 weeks, and sarcopenia was subsequently induced in mice using 20 mg kg^{-1} dexamethasone (DEX) provided i.p. daily for 9 days (Fig. 4A).

In both groups subjected to DEX exposure, a remarkable decrease in body weight was observed in comparison to the normal group (non-DEX-induced groups) (Fig. 4B). Similarly, lean mass exhibited a significant reduction in the DEX group compared to the normal group. However, pretreatment with *L. rhamnosus* IDCC3201 attenuated this reduction in lean mass in the sarcopenia mouse model (Fig. 4C). Furthermore, hand grip force was significantly diminished in the DEX group compared to the normal group, whereas the administration of *L. rhamnosus* IDCC3201 resulted in an improvement in hand grip force (see Fig. 4D). We also evaluated the muscle tissue weight of the quadriceps femoris, gastrocnemius, and tibialis anterior. Notably, the administration of 20 mg kg^{-1} dexamethasone (DEX) did not lead to a decrease in muscle weight, thereby resulting in no significant difference between the three groups in this study (Fig. 4E–G).

As shown in Fig. 5A, histological analysis of the three muscles (quadriceps, gastrocnemius, and tibialis anterior) confirmed an atrophic effect of DEX on the muscle tissue and

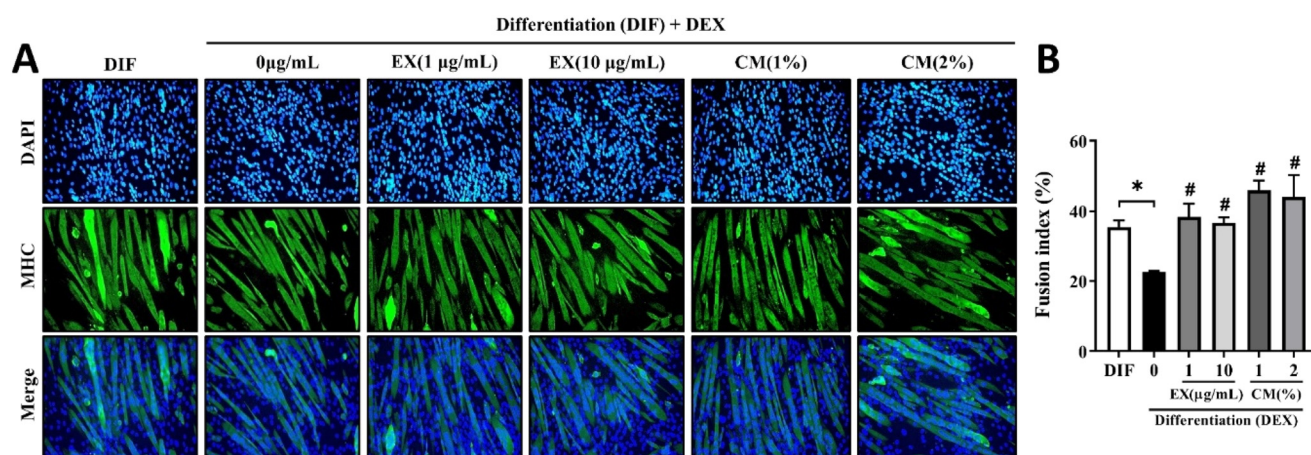


Fig. 2 Upregulated MHC expression in C2C12 myotubes influenced by *L. rhamnosus* IDCC3201. C2C12 myoblasts were cultured over a period of 6 days using differentiation medium (DM) followed by cotreatment with IDCC3201 CM or EX and DEX. (A) Immunofluorescence staining was performed using a mouse anti-MHC primary antibody and an Alexa Fluor 488-conjugated secondary antibody. The nuclei are delineated using DAPI (blue). (B) Evaluation of the myotube fusion index. All data are presented as the mean \pm standard deviation (SD). The width of the myotube was measured using ImageJ software, with values representing the mean and SD derived from 100 individual myotubes. * $P < 0.01$ vs. DIF control. # $P < 0.01$ vs. DIF + DEX positive control.



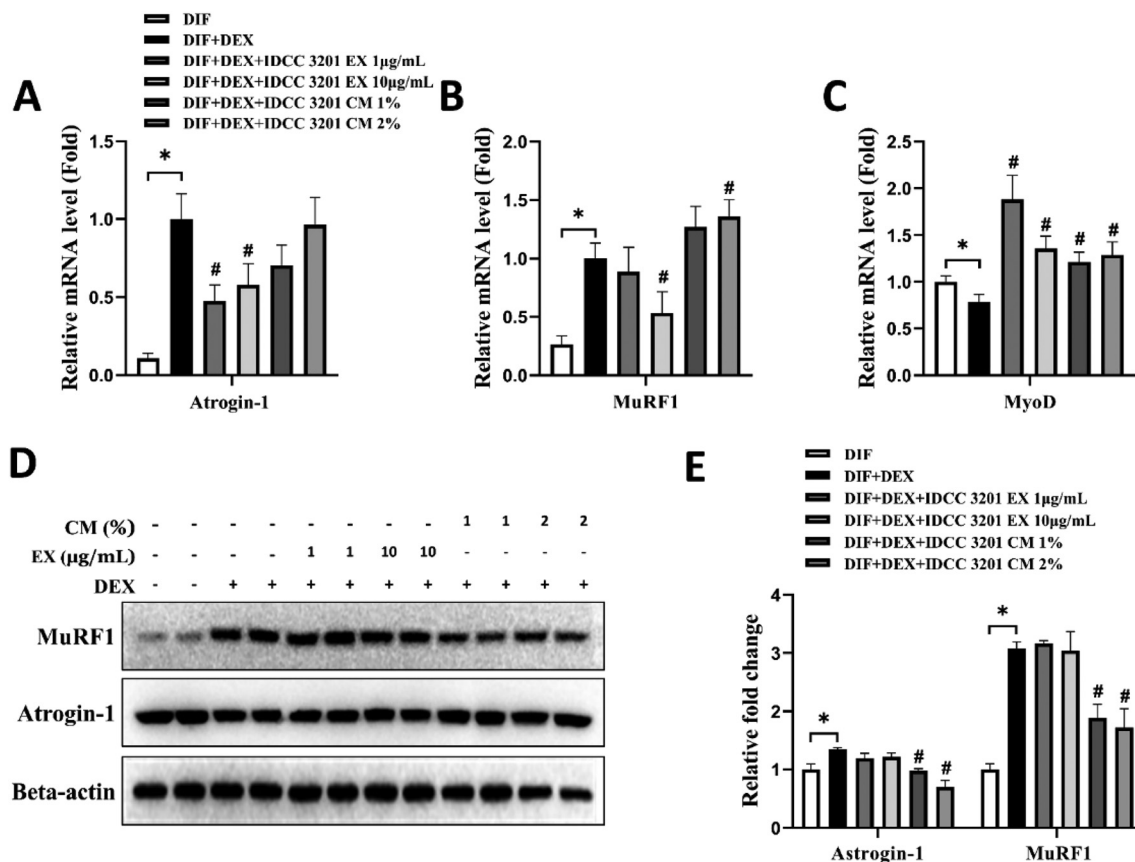


Fig. 3 *L. rhamnosus* IDCC3201 alleviates muscle fiber atrophy in mice through downregulation of E3 ubiquitin ligase expression. (A–C) mRNA expression levels of Atrogin-1, MuRF-1, and MyoD in C2C12 myotube cells were determined using real-time quantitative PCR (RT-qPCR). (D and E) Representative western blot images showcasing the protein expression of Atrogin-1 and MuRF-1 in C2C12 myotube cells. The results derived from both RT-qPCR and western blot analyses are based on three independent replicates ($n = 3$). All data are shown as the mean \pm standard deviation (SD). Statistical significance was determined using an unpaired t test. * $P < 0.05$ vs. DIF. # $P < 0.05$ vs. DIF + DEX. DIF, differentiation negative control; DEX, dexamethasone-treatment positive control; EX, IDCC3201 cell extract; CM, IDCC3201 conditioned medium.

showed that the *L. rhamnosus* IDCC3201 treatment significantly increased the cross-sectional area (CSA). Substantial differences in the size distribution of the three skeletal muscle fibers were also observed (Fig. 5B–D). The area of muscle fibers from more than 3000–3500 μm^2 was more prevalent in the DEX + IDCC3201 group than in the DEX group ($P < 0.001$). The most marked change in muscle fiber size distribution was evident in the gastrocnemius (GC) muscle fibers. As follows median of the muscle fibers: QD; normal (4157 μm^2), DEX (2466 μm^2), DEX + IDCC3201 (3250 μm^2), GC; normal (4152 μm^2), DEX (2120 μm^2), DEX + IDCC3201 (3936 μm^2), TA; normal (4215 μm^2), DEX (2306 μm^2), DEX + IDCC3201 (3139 μm^2) (Fig. 5E–G). These results suggest that *L. rhamnosus* IDCC3201 has the potential to restore the muscle loss observed in DEX-induced muscle sarcopenia mice.

3.4 *L. rhamnosus* IDCC3201 in DEX-induced sarcopenia mice was mitigated by reducing atrophic factors and improving myosin heavy chain

Myosin heavy chain (MHC), which exhibits a variety of isoforms, regulates the metabolism and contractile responses of

skeletal muscles.⁵⁰ Previous studies reported that IL-6 is related to muscle atrophy, and increased IL-6 upregulates the expression of Atrogin-1 and MuRF-1 in skeletal muscle.^{51,52} DEX treatment upregulated the expression of atrophic markers (Atrogin-1, MuRF-1, and myostatin) and the inflammatory cytokine IL-6, but the administration of IDCC3201 restored their expression. Interestingly, a higher myosin heavy chain (MHC1, MHC2A, MHC2B, and MHC2X) was detected in mice in the *L. rhamnosus* IDCC3201 administration group than in the normal group, and DEX treatment reduced the expression of MHC1, MHC2A, MHC2B, and MHC2X. Our results show that *L. rhamnosus* IDCC3201 prevents sarcopenia by inhibiting muscle atrophic factor expression and stimulating myosin heavy chain (MHC) (Fig. 6).

3.5 *L. rhamnosus* IDCC3201 administration affects the gut microbiota composition and metabolism

It has been well established that the gut microbiota not only influences gut health but also impacts the health of various organs. Hence, we assessed the gut microbiome composition of each group of mice and confirmed differences in the



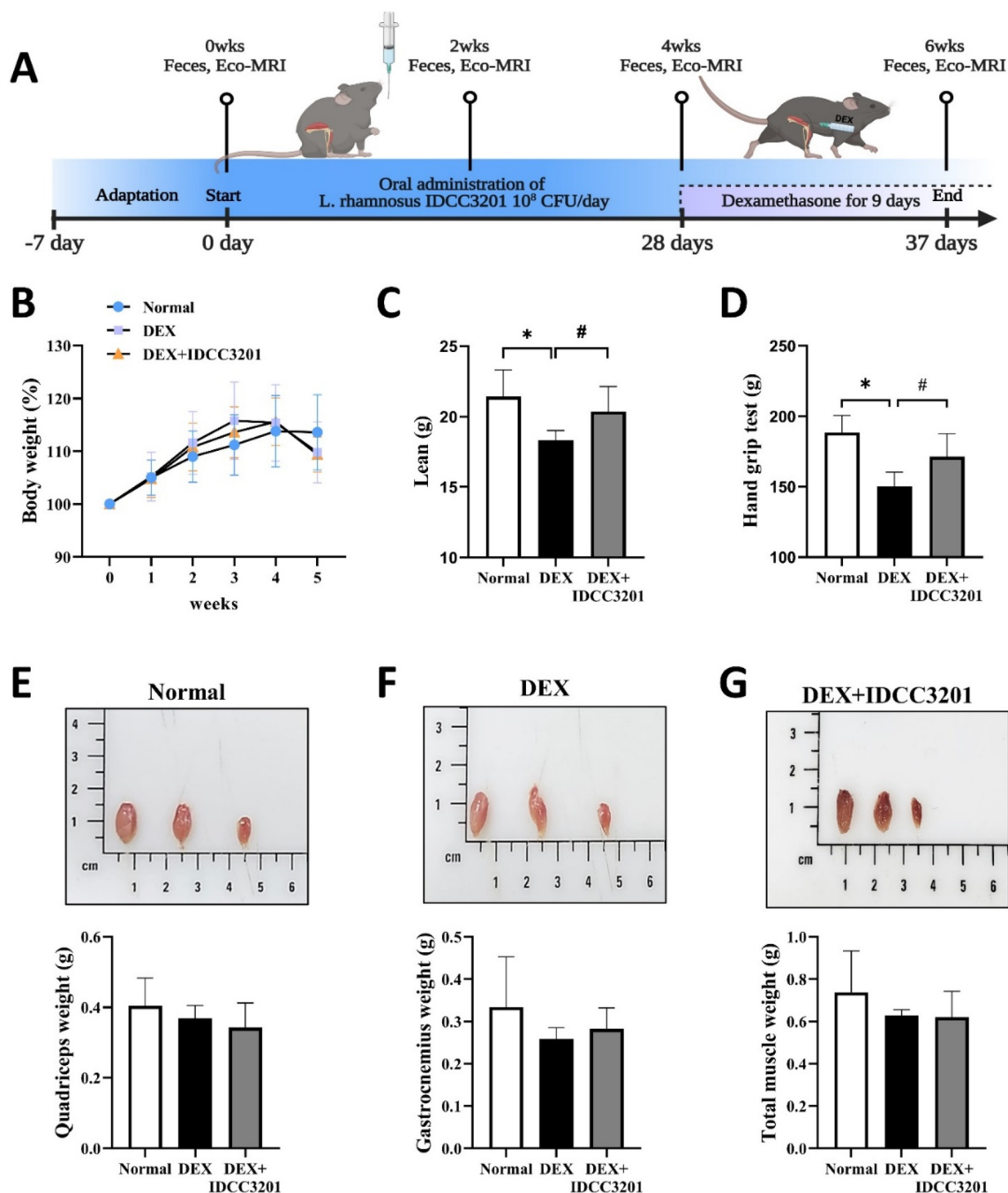


Fig. 4 *L. rhamnosus* IDCC3201 treatment increased lean mass and muscle strength in DEX-administered mice. Seven-week-old male C57BL/6J mice were subjected to an oral administration of IDCC3201 (10^8 CFU per 0.1 mL per mouse per day) for 4 weeks before intraperitoneal injection of DEX (20 mg per kg per day) for 9 days. (A) Schematic diagram of the *in vivo* experimental flow. (B) Mouse body weights were monitored weekly. Prior to euthanization, assessments were made on (C) lean body mass and (D) hand grip strength tests. Mice were sacrificed, and muscle tissues, including (E) quadriceps, (F) gastrocnemius and (G) tibialis anterior, were isolated and subsequently weighed. * $P < 0.01$ vs. normal. # $P < 0.01$ vs. DEX. Data represent the averages from three replicates, and error bars represent standard deviations (SD). Normal, saline control; DEX, DEX-treated positive control; and DEX + IDCC3201 DEX induction with IDCC3201 pretreatment.

microbial taxa. The Chao1, Shannon, and Simpson indices were employed to estimate the richness and alpha diversity of the gut microbiota (Fig. 7A). The results showed that after *L. rhamnosus* IDCC3201 treatment, compared to the DEX group, the Shannon and Simpson indices in the DEX +

IDCC3201 group significantly decreased, whereas the Chao1 index did not considerably change. As shown in Fig. 7B, *Firmicutes* comprised 85.14% (normal group), 75.92% (DEX group), and 78.79% (DEX + IDCC3201 group) of the gut microbiome, and the *Firmicutes/Bacteroidetes* ratio increased in the

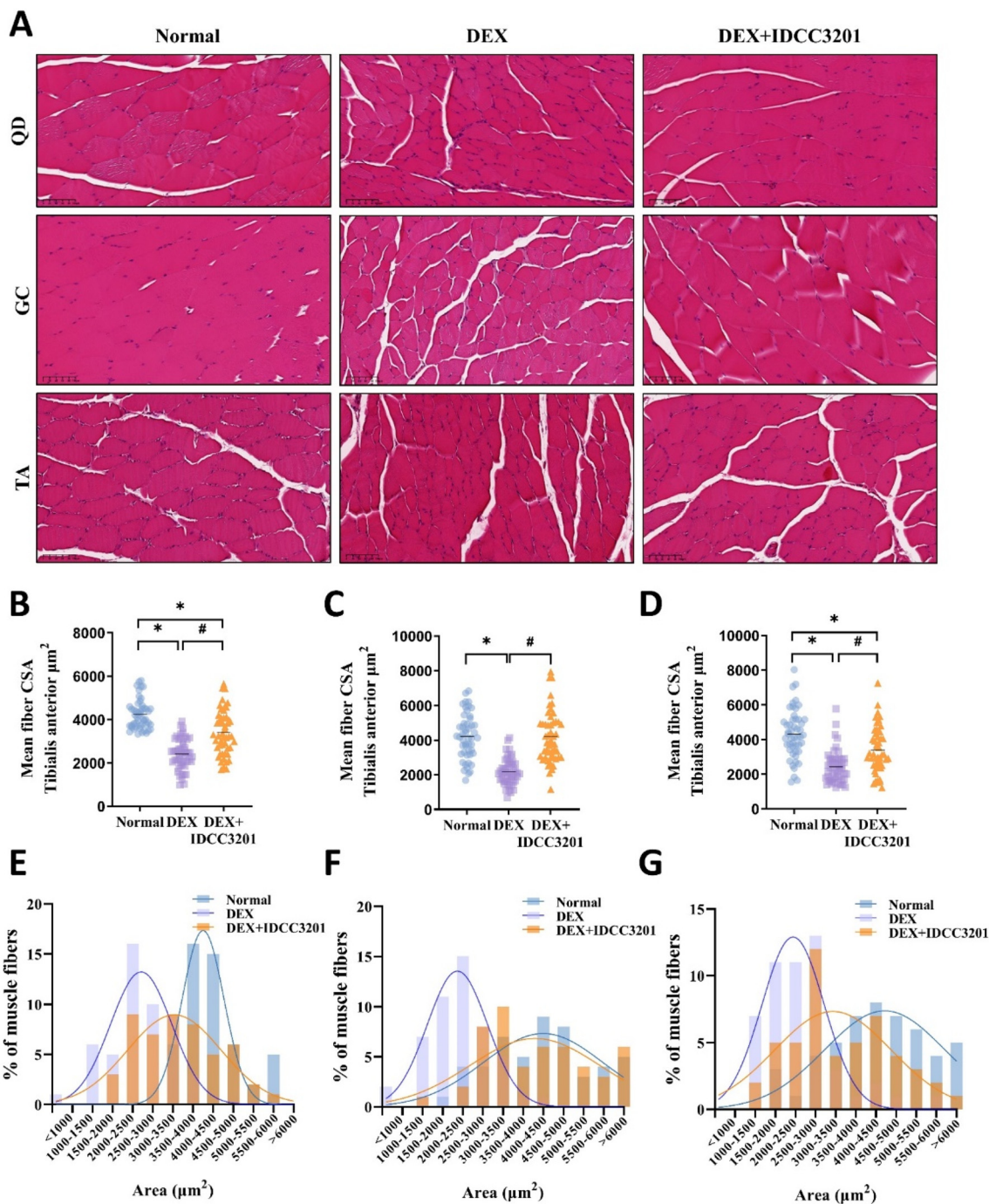


Fig. 5 *L. rhamnosus* IDCC3201 recovers muscle quality in DEX-induced sarcopenia in mice. (A) Muscular tissues from the quadriceps (QD), gastrocnemius (GC), and tibialis anterior (TA) were isolated and subjected to H&E staining and subsequently visualized under microscopy at 20 \times magnification. Using ImageJ software, the cross-sectional area (CSA) of muscle fibers from (B) QD, (C) GC, and (D) TA were quantified. The myofiber size distribution within the (E) QD, (F) GC, and (G) TA muscles for both saline- and IDCC3201-treated mice was delineated. * $P < 0.01$ vs. normal. # $P < 0.01$ vs. DEX. Data represent the averages from three replicates, and error bars represent standard deviations (SD). Normal, saline control; DEX, DEX-treated positive control; and DEX + IDCC3201 DEX induction with IDCC3201 pretreatment.

DEX + IDCC3201 group compared to the DEX group. The sequencing results showed the presence of seven phyla, of which *Firmicutes* and *Bacteroidetes* were the major species. In addition, *Bacteria*, *Proteobacteria*, and *Verrucomicrobia* were present in all three samples (Fig. 7C). Although no significant

changes were observed at the family level and genus level, *Allobaculum* was significantly increased in the *L. rhamnosus* IDCC3201 treatment. In contrast, the populations of lactobacilli exhibited no significant differences among all groups (Fig. 7D and E). Related studies have shown that *Allobaculum*



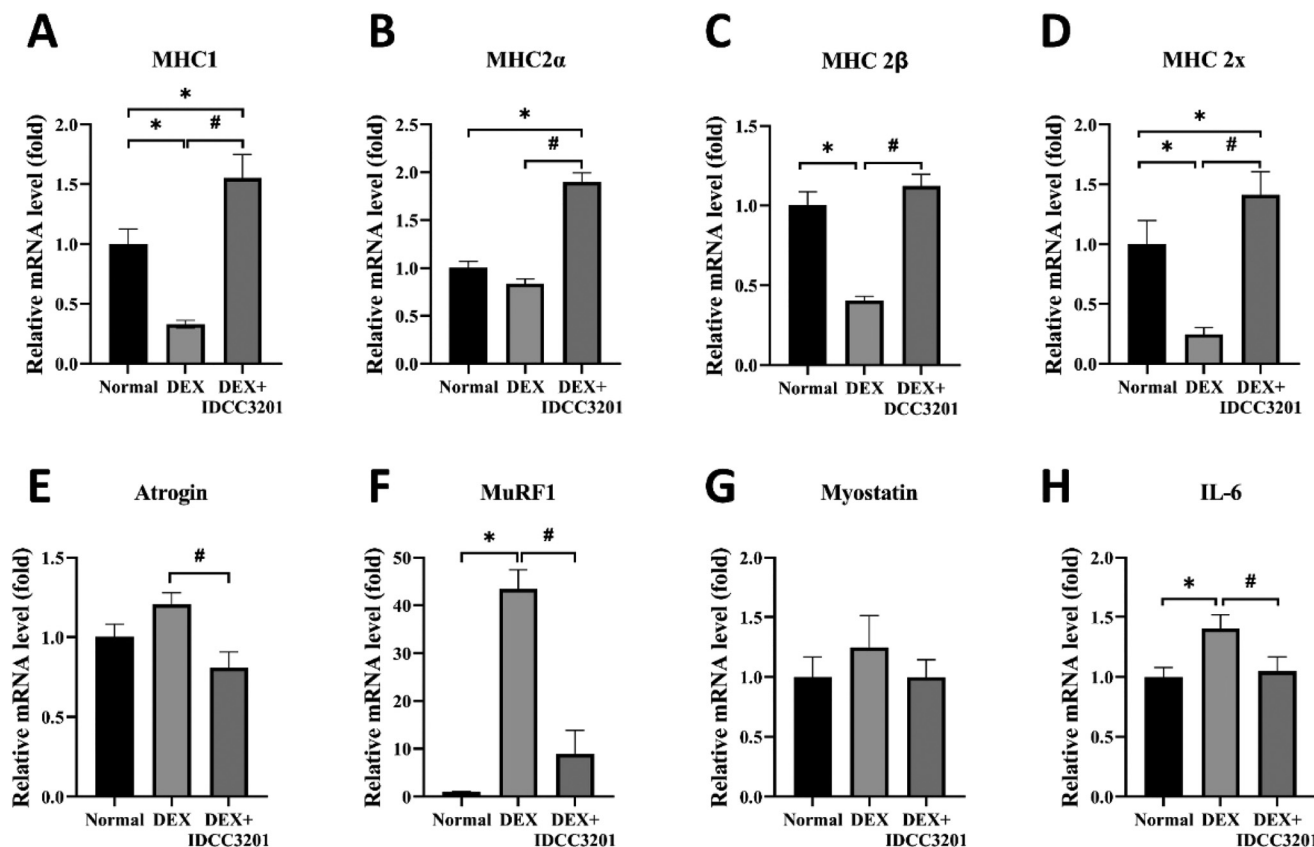


Fig. 6 *L. rhamnosus* IDCC3201 promotes anti-atrophic effects in mice with DEX-induced sarcopenia. (A–D) The mRNA expression of myosin heavy chain (MHC1, MHC 2α, 2β, and 2x) (E–G) atrophy-related factors (Atrogin1, MuRF-1, and myostatin) and (H) proinflammatory cytokines (IL-6) was analyzed using quadriceps (QD) muscle. Statistical analyses comparing differences among the groups were performed using an unpaired *t* test. Statistical significance at **P* < 0.01 vs. normal. #*P* < 0.01 vs. DEX. Data represent the averages from three replicates, and error bars represent standard deviations (SD). Normal, saline control; DEX, DEX-treated positive control; and DEX + IDCC3201 DEX induction with IDCC3201 pretreatment.

can produce butyric acid, modulating intestinal health.⁵³ Therefore, these results suggest that the increase in *Allobaculum* abundance likely alleviates DEX-induced sarcopenia. The genus *Allobaculum* produces short-chain fatty acids (SCFAs). These *Allobaculum*-derived SCFAs have been demonstrated to permeate the systemic circulation, undergo absorption by myocytes, and exert an anti-inflammatory effect.⁵⁴

Next, we investigated the effect of *L. rhamnosus* IDCC3201 administration on gut microbial metabolism using metabolome analysis. Thirty-eight fecal metabolites were specifically identified, including amino acids, branched-chain amino acids (BCAAs), sugars, and free fatty acids. The PCA also suggested that both groups of DEX and DEX + IDCC3201 dramatically shifted the abundance and diversity of metabolites (Fig. 8A). In particular, the shift caused by *L. rhamnosus* IDCC3201 administration was similar to that of the normal group. In particular, the metabolic alterations induced by *L. rhamnosus* IDCC3201 pretreatment were prominently observed in BCAA (L-valine, L-leucine, and L-isoleucine), SCFA (acetic acid and propanoic acid), EFA (essential fatty acids: linoleic acid and oleic acid), and sugar (maltose and D-galactose) (Fig. 8B and C). Therefore, administration of

L. rhamnosus IDCC3201 to DEX-treated mice elicited alterations in metabolite profiles, suggesting an interaction between *L. rhamnosus* IDCC3201 treatment and gut microbiota modulation, particularly affecting the composition of the genus *Allobaculum*.

4. Discussion

Probiotics that provide health benefits to the host have been evaluated in various functional studies, including cognitive behavior, immunomodulation, and anti-inflammatory effects;^{12,55,56} among them, in some lactobacilli, the impact of preventing muscle atrophy or suppressing cachexia has been reported.^{43,57–60} Nonetheless, the influence of probiotic lactobacilli on gut environmental shifts in conjunction with muscle atrophy prevention remains underestimated. The aim of this study was to assess the potential mitigative effects of *L. rhamnosus* IDCC3201 on sarcopenia. Our findings indicate that pretreatment with *L. rhamnosus* IDCC3201 attenuated muscle atrophy in both C2C12 muscle cells and DEX-induced sarcopenia mouse models. We explored whether *L. rhamnosus*



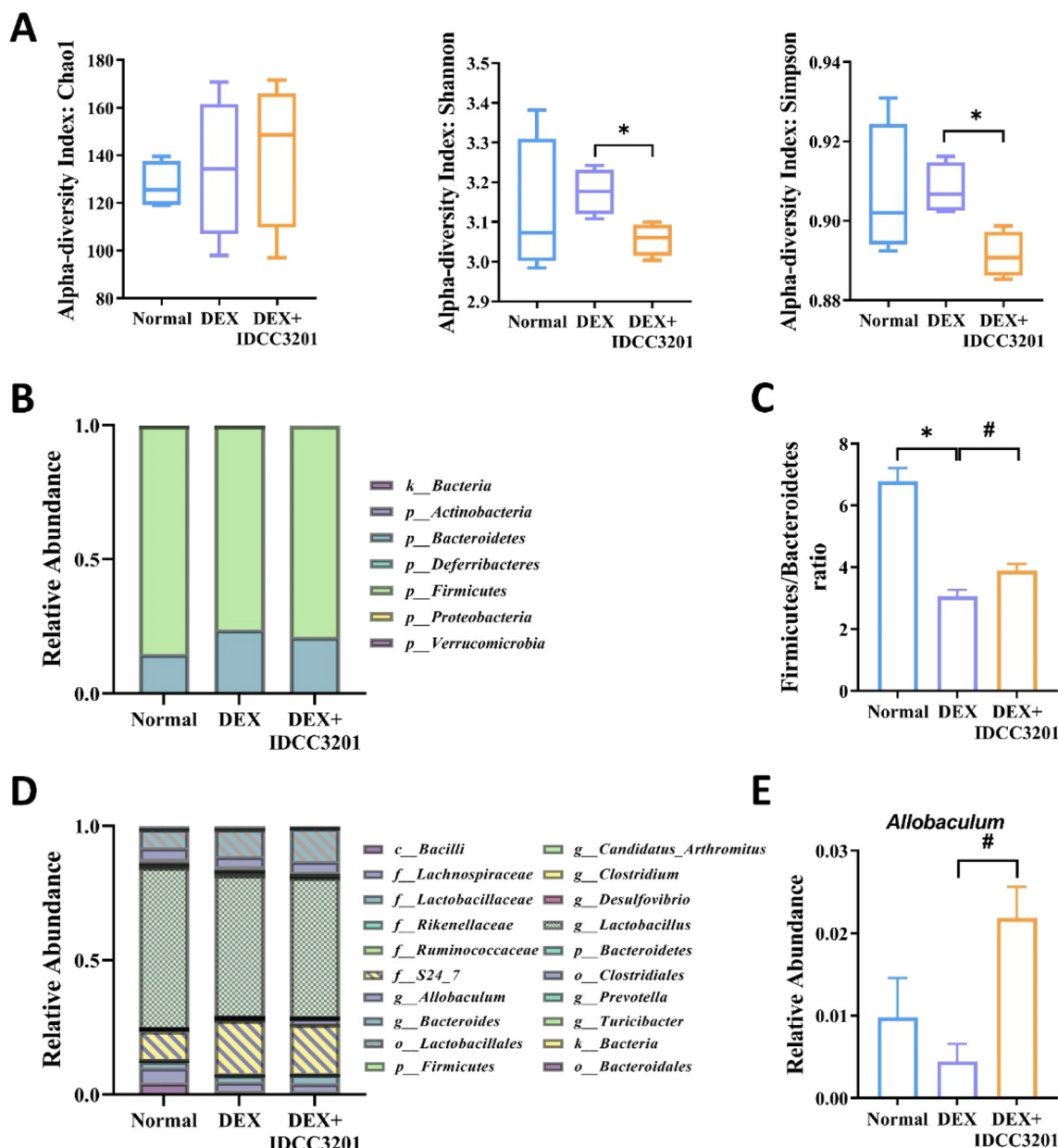


Fig. 7 The fecal microbiota analysis shows a high abundance of *Allobaculum* in *L. rhamnosus* IDCC3201-administered DEX-induced mice. Comparison of α -diversity among groups. (A) The distribution of species richness was measured using the Chao I index (left panel), and the distribution of species evenness was measured using the Shannon (middle panel) index and Simpson (right panel). A horizontal line of the box defines the medians. Whiskers represent the minimum to maximum. (B) Taxonomic composition of fecal microbiota at the phylum level, (C) *Firmicutes* to *Bacteroidetes* ratio, and (D) the genus level. (E) The abundance of *Allobaculum* species in fecal metagenome analysis.

IDCC3201 administration alters the gut microbial composition and modulates metabolite profiles. The administration of IDCC3201 fundamentally influenced the metabolite profile as well as gut microbiota composition, significantly augmenting the population of *Allobaculum*, an SCFA-producing bacterium, in sarcopenic mice. The fecal metabolomics analysis revealed that enhanced BCAA, SCFA, sugar, and essential fatty acid-relevant organic acids collaborate with alterations in gut bacterial composition. The results obtained in our study suggest that the possible anti-atrophy effects of *L. rhamnosus* IDCC3201 in

sarcopenia are associated with changes in the gut microbiota and subsequent metabolite production.

Several investigations have established that dexamethasone (DEX) instigates sarcopenia in murine models by accelerating proteolytic activity and particularly targeting type II muscle fibers, thus mimicking the muscle degradation observed in age-related sarcopenia.^{61–63} Accordingly, to simulate muscle atrophy, dexamethasone was subsequently employed both *in vitro* and *in vivo*. The C2C12 myoblast cell line, mononuclear cells that fused into thickened, multinucleated myotubes

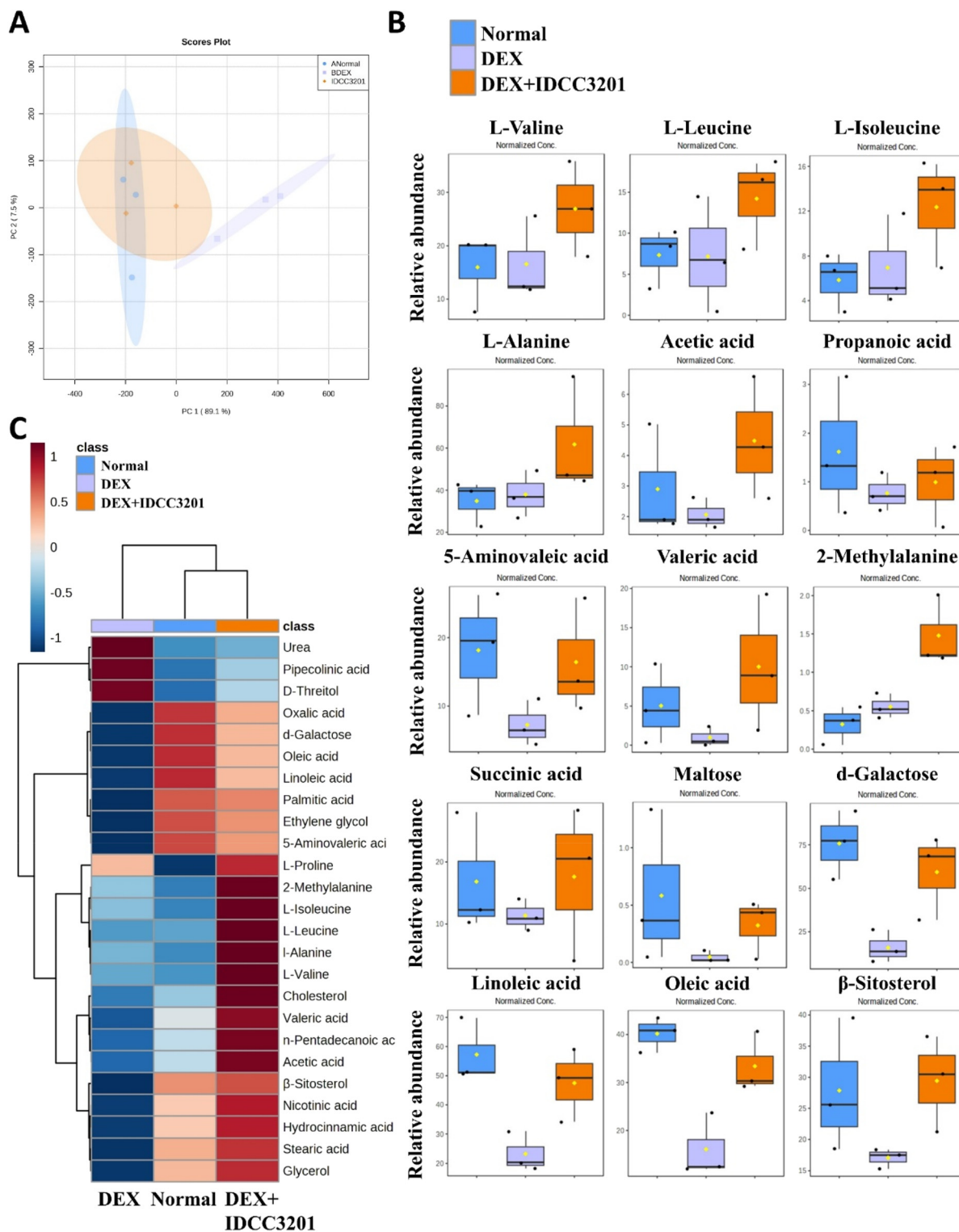


Fig. 8 Analysis of fecal metabolite changes in a sarcopenia mouse following *L. rhamnosus* IDCC3201 administration. (A) Principal component analysis (PCA) displays variations in the relative abundance of fifteen specific metabolites. (B) Boxplots of key metabolic compounds, including BCAAs (L-valine, L-leucine, and L-isoleucine), SCFAs (acetic acid and propanoic acid), EFAs (linoleic acid and oleic acid), and sugars (maltose and D-galactose), highlighting the metabolic shifts induced by the IDCC3201 treatment. (C) Clustering heat-map analysis of the top 25 families, revealing distinct group separation. The color gradient in the heatmap highlights the relative metabolite content: red for higher and blue for lower concentrations.



during differentiation, is prevalently employed in muscle-related research.^{64–66} As myoblasts differentiate, the cell phenotype changes to a myocyte with an abundance of protein structures, and the expression of various differentiation markers (MHC; myosin heavy chain, MyoD, α -actin, and myogenin) is upregulated.^{64,67} As shown in Fig. 2 and 3, *L. rhamnosus* IDCC3201 alleviated myotube atrophy and increased the expression of MHC and the fusion index of DEX-treated differentiated myoblasts. Previous studies reported that dexamethasone (DEX) caused diminished protein synthesis and increased degradation, resulting in increased expression of Atrogin-1 and MuRF-1, concurrent with inhibited phosphorylation of the PI3K/AKT/FoxO3a pathway.^{68–70} Remarkably, our observations were consistent with these findings concerning the inhibition of muscle atrophy. Dietary supplementation with *L. rhamnosus* IDCC3201 significantly prevented the muscle atrophy response induced by DEX. In addition, we confirmed that DEX administration markedly decreased MHCI and MHCII (a, b, and x) and increased, as expected, the expression of Atrogin-1, MuRF-1, and myostatin. However, treatment with *L. rhamnosus* IDCC3201 significantly increased the mRNA expression levels of MHCI and MHCII. Consequently, it attenuated the expression of these atrophic muscle factors, indicating that *L. rhamnosus* IDCC3201 may confer protection to muscle fibers against DEX-induced damage. Currently, our ongoing study is elucidating the

specific inhibitory mechanism for the muscle atrophy of *L. rhamnosus* IDCC3201 at the molecular level.

Skeletal muscle is composed of two primary fiber types: slow-twitch (type I) and fast-twitch (type II),^{71,72} and there are four isoforms (MHC I, MHC IIa, b, and x).⁷³ Muscle atrophy due to aging causes a decrease in fast-twitch (type II) muscle fibers, similar to when DEX is induced.^{71,74} Kohn *et al.*⁷⁵ reported that all four MHC isoforms were identified in QD in rat skeletal muscle, and MHC IIb and MHC IIX were most frequently detected. To confirm the muscle improvement effect, we selected QD among the three sampled muscles (QD, GC, and TA). In this study, we demonstrated decreased CSA and four MHC isoforms and upregulated Atrogin-1, MuRF-1, and myostatin by DEX administration. *L. rhamnosus* IDCC3201 positively regulated this atrophic response, and the increased expression of IL-6 due to DEX was significantly reduced, consistent with previous reports.^{51,52}

Aging impairs intestinal function and induces alterations in the gut microbiome composition.^{76–80} O'Toole P. W. and Vaiserman A. M. reported a high ratio of *Firmicutes/Bacteroidetes* in elderly compared to young subjects.^{81,82} Shifts in the gut microbiome composition have been implicated in modifying the host metabolic phenotype, thereby exerting a considerable influence on age-associated disorders.^{80,83} Chevalier and colleagues confirmed that temperature is a determinant influencing microbiome changes and observed

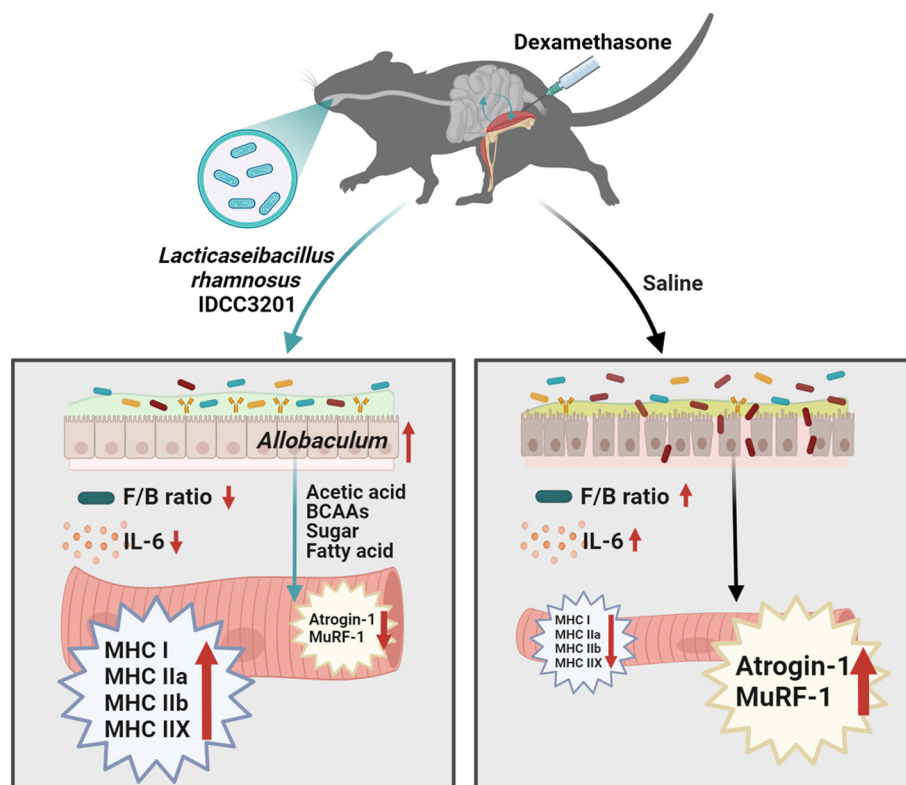


Fig. 9 Schematic diagram. This schematic provides an overview of the influence of *L. rhamnosus* IDCC3201 on the skeletal muscle atrophy process, affecting metabolomic and gut microbiome alterations. Graphics were created with BioRender.com.



an expedited browning of white adipose tissue following the transplantation of gut microbiota from cold-adapted mice into a control group.⁸⁴ Therefore, the gut microbiome composition is important in preventing metabolic disease. Our results showed that the *Firmicutes/Bacteroidetes* ratio altered by DEX treatment was significantly restored by the administration of *L. rhamnosus* IDCC3201.

Despite the lack of biochemical and genetic characteristics of the genus *Allobaculum*, they are recognized as producers of SCFAs, predominantly acetic acid, and are implicated in fatty acid metabolism and aging-related processes.^{30,85–87} Yang Z. *et al.* suggested that supplementation with a BCAA-enriched mixture significantly altered gut microbiota age-related compositional changes and gut metabolism, such as fructose, sucrose, and oleic acid.⁸⁸ In addition, dietary essential amino acids (EAAs) have been reported to regulate the intestinal immune system through their role in protein synthesis^{89–92} and to promote skeletal muscle mitochondria generation⁹³ and muscle protein synthesis.⁸⁸ Taken together, gut metabolites such as BCAAs and EAAs can directly affect tissues such as muscle by regulating metabolism and energy balance.^{80,94}

In the current investigation, the therapeutic efficacy of live probiotics in mitigating muscle atrophy was evaluated through oral administration in murine models. However, for *in vitro* evaluation, it was imperative to prepare CM and EX independently and administer them to myogenic differentiated cells. Considering the established effectiveness of exopolysaccharides (EPS) as bioactive components with health-promoting properties,⁹⁵ the isolation and quantification of EPS were conducted based on our previous research.⁹⁶ The released EPS within CM and cell-bound EPS within EX were successfully separated, allowing future exploration of cellular molecular mechanisms and modulation of gut microbiome, affecting producing their metabolites.

5. Conclusion

Our present findings provide excellent insights into the efficacy of *L. rhamnosus* IDCC3201 targeting acetic acid and BCAA to induce significant production, thereby encouraging benefits for intestinal health and alleviating sarcopenia, suggesting the need for further definite mechanistic studies. In conclusion, *L. rhamnosus* IDCC3201 demonstrates protective effects against muscle atrophy in DEX-induced sarcopenia as a therapeutic dietary supplement (Fig. 9).

Data availability

Data will be made available on request.

Author contributions

Minkyung Kang, Minji Kang, Jisun Yoo, Juyeon Lee, Sujeong Lee, Bohyun Yun, Minho Song, Jun-Mo Kim, Hyung Wook

Kim, Jungwoo Yang, Younghoon Kim, and Sangnam Oh: writing – original draft, investigation; Minji Kang, Jisun Yoo, Juyeon Lee, Sujeong Lee, Minho Song, Jun-Mo Kim, Hyung Wook Kim, Jungwoo Yang: methodology, validation; Younghoon Kim, and Sangnam Oh: conceptualization, resources, funding acquisition, writing – review & editing.

Conflicts of interest

The authors state no potential conflicts of interest.

Acknowledgements

This study was supported by the Korea Institute of Planning and Evaluation for Technology in Food, Agriculture, Forestry and Fisheries (IPET-321037-5) and by a National Research Foundation of Korea Grant funded by the Korean government (MEST) (NRF-2021R1A2C3011051).

References

- 1 S. Schiaffino, K. A. Dyar, S. Ciciliot, B. Blaauw and M. Sandri, Mechanisms regulating skeletal muscle growth and atrophy, *FEBS J.*, 2013, **280**, 4294–4314.
- 2 J. Y. Kim, H. M. Kim, J. H. Kim, J. H. Lee, K. Zhang, S. Guo, D. H. Lee, E. M. Gao, R. H. Son, S. M. Kim and C. Y. Kim, Preventive effects of the butanol fraction of *Justicia procumbens* L. against dexamethasone-induced muscle atrophy in C2C12 myotubes, *Heliyon*, 2022, **8**, e11597.
- 3 K. Lenk, G. Schuler and V. Adams, Skeletal muscle wasting in cachexia and sarcopenia: molecular pathophysiology and impact of exercise training, *J. Cachexia Sarcopenia Muscle*, 2010, **1**, 9–21.
- 4 C. L. Cole, I. R. Kleckner, A. Jatoti, E. M. Schwarz and R. F. Dunne, The role of systemic inflammation in cancer-associated muscle wasting and rationale for exercise as a therapeutic intervention, *JCSM Clin. Rep.*, 2018, **3**, 1–19.
- 5 S. J. van Krimpen, F. A. C. Jansen, V. L. Ottenheim, C. Belzer, M. van der Ende and K. van Norren, The Effects of Pro-, Pre-, and Synbiotics on Muscle Wasting, a Systematic Review-Gut Permeability as Potential Treatment Target, *Nutrients*, 2021, **13**(4), 1115.
- 6 A. Picca, F. Fanelli, R. Calvani, G. Mule, V. Pesce, A. Sisto, C. Pantanelli, R. Bernabei, F. Landi and E. Marzetti, Gut Dysbiosis and Muscle Aging: Searching for Novel Targets against Sarcopenia, *Mediators Inflammation*, 2018, **2018**, 7026198.
- 7 E. Marzetti, R. Calvani, M. Tosato, M. Cesari, M. Di Bari, A. Cherubini, A. Collamati, E. D'Angelo, M. Pahor, R. Bernabei, F. Landi and S. Consortium, Sarcopenia: an overview, *Aging: Clin. Exp. Res.*, 2017, **29**, 11–17.
- 8 H. J. Kang and S. H. Im, Probiotics as an Immune Modulator, *J. Nutr. Sci. Vitaminol.*, 2015, **61**, S103–S105.



- 9 H. Chung, S. J. Pamp, J. A. Hill, N. K. Surana, S. M. Edelman, E. B. Troy, N. C. Reading, E. J. Villablanca, S. Wang, J. R. Mora, Y. Umesaki, D. Mathis, C. Benoist, D. A. Relman and D. L. Kasper, Gut immune maturation depends on colonization with a host-specific microbiota, *Cell*, 2012, **149**, 1578–1593.
- 10 M. Schwarzer, K. Makki, G. Storelli, I. Machuca-Gayet, D. Srutkova, P. Hermanova, M. E. Martino, S. Balmand, T. Hudcovic, A. Heddi, J. Rieusset, H. Kozakova, H. Vidal and F. Leulier, Lactobacillus plantarum strain maintains growth of infant mice during chronic undernutrition, *Science*, 2016, **351**, 854–857.
- 11 M. Kang, H. J. Choi, B. Yun, J. Lee, J. Yoo, H.-J. Yang, D.-Y. Jeong, Y. Kim and S. Oh, Bacillus amyloliquefaciens SCGB1 Alleviates Dextran Sulfate Sodium-Induced Colitis in Mice Through Immune Regulation, *J. Med. Food*, 2021, **24**, 709–719.
- 12 M. R. Park, M. Shin, D. Mun, S. Y. Jeong, D. Y. Jeong, M. Song, G. Ko, T. Unno, Y. Kim and S. Oh, Probiotic Lactobacillus fermentum strain JDFM216 improves cognitive behavior and modulates immune response with gut microbiota, *Sci. Rep.*, 2020, **10**, 21701.
- 13 S. Gu, D. Yang, C. Liu and W. Xue, The role of probiotics in prevention and treatment of food allergy, *Food Sci. Hum. Wellness*, 2023, **12**, 681–690.
- 14 M. H. Jaafar, P. Xu, U. M. Mageswaran, S. D. Balasubramaniam, M. Solayappan, J. J. Woon, C. S. J. Teh, S. D. Todorov, Y. H. Park, G. Liu and M. T. Liong, Constipation anti-aging effects by dairy-based lactic acid bacteria, *J. Anim. Sci. Technol.*, 2024, **66**, 178–203.
- 15 K. Jeon, M. Song, J. Lee, H. Oh, S. Chang, D. Song, J. An, H. Cho, S. Park, H. Kim and J. Cho, Effects of Single and Complex Probiotics in Growing-Finishing Pigs and Swine Compost, *J. Anim. Sci. Technol.*, 2023, DOI: [10.5187/jast.2023.e88](https://doi.org/10.5187/jast.2023.e88).
- 16 D. Lee, T. W. Goh, M. G. Kang, H. J. Choi, S. Y. Yeo, J. Yang, C. S. Huh, Y. Y. Kim and Y. Kim, Perspectives and advances in probiotics and the gut microbiome in companion animals, *J. Anim. Sci. Technol.*, 2022, **64**, 197–217.
- 17 D. Song, J. Lee, Y. Yoo, H. Oh, S. Chang, J. An, S. Park, K. Jeon, Y. Cho, Y. Yoon and J. Cho, Effects of probiotics on growth performance, intestinal morphology, intestinal microbiota weaning pig challenged with Escherichia coli and Salmonella enterica, *J. Anim. Sci. Technol.*, 2023, DOI: [10.5187/jast.2023.e119](https://doi.org/10.5187/jast.2023.e119).
- 18 R. Vasquez, J. K. Oh, J. H. Song and D. K. Kang, Gut microbiome-produced metabolites in pigs: a review on their biological functions and the influence of probiotics, *J. Anim. Sci. Technol.*, 2022, **64**, 671–695.
- 19 S. A. Chae, S. R. Ramakrishnan, T. Kim, S. R. Kim, W. Y. Bang, C. R. Jeong, J. Yang and S. J. Kim, Anti-inflammatory and anti-pathogenic potential of Lactobacillus rhamnosus IDCC 3201 isolated from feces of breast-fed infants, *Microb. Pathog.*, 2022, **173**, 105857.
- 20 N. S. Oh, J. Y. Joung, J. Y. Lee and Y. Kim, Probiotic and anti-inflammatory potential of Lactobacillus rhamnosus 4B15 and Lactobacillus gasseri 4M13 isolated from infant feces, *PLoS One*, 2018, **13**, e0192021.
- 21 T. Wang, H. Yan, Y. Lu, X. Li, X. Wang, Y. Shan, Y. Yi, B. Liu, Y. Zhou and X. Lu, Anti-obesity effect of Lactobacillus rhamnosus LS-8 and Lactobacillus crustorum MN047 on high-fat and high-fructose diet mice base on inflammatory response alleviation and gut microbiota regulation, *Eur. J. Nutr.*, 2020, **59**, 2709–2728.
- 22 A. Kumari, S. Bhawal, S. Kapila and R. Kapila, Probiotic lactobacilli mediate their immunoregulatory functions in intestinal cells via modulation of H3 histone acetylation, *J. Appl. Microbiol.*, 2022, **134**, lxac045.
- 23 X. Miao, Y. Jiang, D. Kong, Z. Wu, H. Liu, X. Ye and W. Gong, Lactobacillus rhamnosus HN001 Ameliorates BEZ235-Induced Intestinal Dysbiosis and Prolongs Cardiac Transplant Survival, *Microbiol. Spectrum*, 2022, **10**, e0079422.
- 24 S. Yeo, H. Park, E. Seo, J. Kim, B. K. Kim, I. S. Choi and C. S. Huh, Anti-Inflammatory and Gut Microbiota Modulatory Effect of Lactobacillus rhamnosus Strain LDTM 7511 in a Dextran Sulfate Sodium-Induced Colitis Murine Model, *Microorganisms*, 2020, **8**, 845.
- 25 L. Bonfrate, D. M. Di Palo, G. Celano, A. Albert, P. Vitellio, M. De Angelis, M. Gobetti and P. Portincasa, Effects of Bifidobacterium longum BB536 and Lactobacillus rhamnosus HN001 in IBS patients, *Eur. J. Clin. Invest.*, 2020, **50**, e13201.
- 26 S. Lee, J. Kang and D. Kang, Anti-allergic effect of Lactobacillus rhamnosus IDCC 3201 isolated from breast milk-fed Korean infant, *Korean J. Microbiol.*, 2016, **52**, 18–24.
- 27 S. H. Lee, J. M. Yoon, Y. H. Kim, D. G. Jeong, S. Park and D. J. Kang, Therapeutic effect of tyndallized Lactobacillus rhamnosus IDCC 3201 on atopic dermatitis mediated by down-regulation of immunoglobulin E in NC/Nga mice, *Microbiol. Immunol.*, 2016, **60**, 468–476.
- 28 M. Giron, M. Thomas, D. Dardevet, C. Chassard and I. Savary-Auzeloux, Gut microbes and muscle function: can probiotics make our muscles stronger?, *J. Cachexia Sarcopenia Muscle*, 2022, **13**, 1460–1476.
- 29 A. Ticinesi, A. Nouvenne, N. Cerundolo, P. Catania, B. Prati, C. Tana and T. Meschi, Gut microbiota, muscle mass and function in aging: a focus on physical frailty and sarcopenia, *Nutrients*, 2019, **11**, 1633.
- 30 H. L. Greetham, G. R. Gibson, C. Giffard, H. Hippe, B. Merkhoffer, U. Steiner, E. Falsen and M. D. Collins, Allobaculum stercoricanis gen. nov., sp. nov., isolated from canine feces, *Anaerobe*, 2004, **10**, 301–307.
- 31 A. Ticinesi, F. Lauretani, C. Milani, A. Nouvenne, C. Tana, D. Del Rio, M. Maggio, M. Ventura and T. Meschi, Aging gut microbiota at the cross-road between nutrition, physical frailty, and sarcopenia: is there a gut–muscle axis?, *Nutrients*, 2017, **9**, 1303.
- 32 M. S. Lustgarten, The Role of the Gut Microbiome on Skeletal Muscle Mass and Physical Function: 2019 Update, *Front. Physiol.*, 2019, **10**, 1435.



- 33 A. M. Davila, F. Blachier, M. Gotteland, M. Andriamihaja, P. H. Benetti, Y. Sanz and D. Tome, Intestinal luminal nitrogen metabolism: role of the gut microbiota and consequences for the host, *Pharmacol. Res.*, 2013, **68**, 95–107.
- 34 T. Hashimoto, T. Perlot, A. Rehman, J. Trichereau, H. Ishiguro, M. Paolino, V. Sigl, T. Hanada, R. Hanada, S. Lipinski, B. Wild, S. M. Camargo, D. Singer, A. Richter, K. Kuba, A. Fukamizu, S. Schreiber, H. Clevers, F. Verrey, P. Rosenstiel and J. M. Penninger, ACE2 links amino acid malnutrition to microbial ecology and intestinal inflammation, *Nature*, 2012, **487**, 477–481.
- 35 J. Frampton, K. G. Murphy, G. Frost and E. S. Chambers, Short-chain fatty acids as potential regulators of skeletal muscle metabolism and function, *Nat. Metab.*, 2020, **2**, 840–848.
- 36 K. Yamanashi, S. Kinugawa, A. Fukushima, N. Kakutani, S. Takada, Y. Obata, I. Nakano, T. Yokota, Y. Kitauro, Y. Shimomura and T. Anzai, Branched-chain amino acid supplementation ameliorates angiotensin II-induced skeletal muscle atrophy, *Life Sci.*, 2020, **250**, 117593.
- 37 Y. S. Nanjundaiah, D. A. Wright, A. R. Baydoun, W. T. O'Hare, Z. Ali, Z. Khaled and M. H. Sarker, *Lactobacillus rhamnosus* GG conditioned media modulates acute reactive oxygen species and nitric oxide in J774 murine macrophages, *Biochem. Biophys. Rep.*, 2016, **6**, 68–75.
- 38 P. Velica and C. M. Bunce, A quick, simple and unbiased method to quantify C2C12 myogenic differentiation, *Muscle Nerve*, 2011, **44**, 366–370.
- 39 S. Ryu, H. Kyoung, K. I. Park, S. Oh, M. Song and Y. Kim, Postbiotic heat-killed lactobacilli modulates on body weight associated with gut microbiota in a pig model, *AMB Express*, 2022, **12**, 83.
- 40 P. D. Schloss, S. L. Westcott, T. Ryabin, J. R. Hall, M. Hartmann, E. B. Hollister, R. A. Lesniewski, B. B. Oakley, D. H. Parks, C. J. Robinson, J. W. Sahl, B. Stres, G. G. Thallinger, D. J. Van Horn and C. F. Weber, Introducing mothur: open-source, platform-independent, community-supported software for describing and comparing microbial communities, *Appl. Environ. Microbiol.*, 2009, **75**, 7537–7541.
- 41 J. Chong, P. Liu, G. Zhou and J. Xia, Using MicrobiomeAnalyst for comprehensive statistical, functional, and meta-analysis of microbiome data, *Nat. Protoc.*, 2020, **15**, 799–821.
- 42 K. Oliphant and E. Allen-Vercoe, Macronutrient metabolism by the human gut microbiome: major fermentation by-products and their impact on host health, *Microbiome*, 2019, **7**, 1–15.
- 43 C. Liu, W. H. Cheung, J. Li, S. K. Chow, J. Yu, S. H. Wong, M. Ip, J. J. Y. Sung and R. M. Y. Wong, Understanding the gut microbiota and sarcopenia: a systematic review, *J. Cachexia Sarcopenia Muscle*, 2021, **12**, 1393–1407.
- 44 M. Y. Lin and C. L. Yen, Antioxidative ability of lactic acid bacteria, *J. Agric. Food Chem.*, 1999, **47**, 1460–1466.
- 45 R. Gyawali, A. Oyeniran, T. Zimmerman, S. O. Aljaloud, A. Krastanov and S. A. Ibrahim, A comparative study of extraction techniques for maximum recovery of beta-galactosidase from the yogurt bacterium *Lactobacillus delbrueckii* ssp. *bulgaricus*, *J. Dairy Res.*, 2020, **87**, 123–126.
- 46 A. Burgut, Growth inhibition of foodborne pathogens by co-microencapsulation of lactobacilli cell free and propolis extracts, *J. Food Saf.*, 2021, **41**, e12863.
- 47 B. H. Nataraj, S. A. Ali, P. V. Behare and H. Yadav, Postbiotics-parabiotics: the new horizons in microbial biotherapy and functional foods, *Microb. Cell Fact.*, 2020, **19**, 168.
- 48 S. Haberecht-Muller, E. Kruger and J. Fielitz, Out of Control: The Role of the Ubiquitin Proteasome System in Skeletal Muscle during Inflammation, *Biomolecules*, 2021, **11**, 1327.
- 49 J. P. Gumucio and C. L. Mendias, Atrogin-1, MuRF-1, and sarcopenia, *Endocrine*, 2013, **43**, 12–21.
- 50 M. Hashimoto, T. Inoue, M. Katakura, S. Hossain, A. A. Mamun, K. Matsuzaki, H. Arai and O. Shido, Differential effects of docosahexaenoic and arachidonic acid on fatty acid composition and myosin heavy chain-related genes of slow- and fast-twitch skeletal muscle tissues, *Mol. Cell. Biochem.*, 2016, **415**, 169–181.
- 51 L. Pelosi, M. G. Berardinelli, L. Forcina, F. Ascenzi, E. Rizzuto, M. Sandri, F. De Benedetti, B. M. Scicchitano and A. Musaro, Sustained Systemic Levels of IL-6 Impinge Early Muscle Growth and Induce Muscle Atrophy and Wasting in Adulthood, *Cells*, 2021, **10**, 1816.
- 52 L. Zhang, J. Du, Z. Hu, G. Han, P. Delafontaine, G. Garcia and W. E. Mitch, IL-6 and serum amyloid A synergy mediates angiotensin II-induced muscle wasting, *J. Am. Soc. Nephrol.*, 2009, **20**, 604–612.
- 53 Z. Zheng, W. Lyu, Y. Ren, X. Li, S. Zhao, H. Yang and Y. Xiao, Allobaculum Involves in the Modulation of Intestinal ANGPTL4 Expression in Mice Treated by High-Fat Diet, *Front. Nutr.*, 2021, **8**, 690138.
- 54 Q. Yuan, B. Zhan, R. Chang, M. Du and X. Mao, Antidiabetic Effect of Casein Glycomacropeptide Hydrolysates on High-Fat Diet and STZ-Induced Diabetic Mice via Regulating Insulin Signaling in Skeletal Muscle and Modulating Gut Microbiota, *Nutrients*, 2020, **12**, 220.
- 55 M. Kang, H. J. Choi, B. Yun, J. Lee, J. Yoo, H. J. Yang, D. Y. Jeong, Y. Kim and S. Oh, *Bacillus amyloliquefaciens* SCGB1 Alleviates Dextran Sulfate Sodium-Induced Colitis in Mice Through Immune Regulation, *J. Med. Food*, 2021, **24**, 709–719.
- 56 B. A. Tegegne and B. Kebede, Probiotics, their prophylactic and therapeutic applications in human health development: A review of the literature, *Heliyon*, 2022, **8**(6), e09725.
- 57 H. Izumi, N. Kosaka, T. Shimizu, K. Sekine, T. Ochiya and M. Takase, Time-dependent expression profiles of microRNAs and mRNAs in rat milk whey, *PLoS One*, 2014, **9**, e88843.
- 58 L. H. Chen, S. S. Chang, H. Y. Chang, C. H. Wu, C. H. Pan, C. C. Chang, C. H. Chan and H. Y. Huang, Probiotic supplementation attenuates age-related sarcopenia via the gut-muscle axis in SAMP8 mice, *J. Cachexia Sarcopenia Muscle*, 2022, **13**, 515–531.



- 59 H. Jeon, Y. T. Kim, W. Y. Jang, J. Y. Kim, K. Heo, J. J. Shim, J. L. Lee, D. C. Yang and S. C. Kang, Effects of *Lactobacillus curvatus* HY7602-Fermented Antlers in Dexamethasone-Induced Muscle Atrophy, *Fermentation*, 2022, **8**, 454.
- 60 K. Lee, J. Kim, S. D. Park, J. J. Shim and J. L. Lee, *Lactobacillus plantarum* HY7715 Ameliorates Sarcopenia by Improving Skeletal Muscle Mass and Function in Aged Balb/c Mice, *Int. J. Mol. Sci.*, 2021, **22**, 10023.
- 61 W. Q. Xie, M. He, D. J. Yu, Y. X. Wu, X. H. Wang, S. Lv, W. F. Xiao and Y. S. Li, Mouse models of sarcopenia: classification and evaluation, *J. Cachexia Sarcopenia Muscle*, 2021, **12**, 538–554.
- 62 C. S. Chiu, H. Weber, S. Adamski, A. Rauch, M. A. Gentile, S. E. Alves, G. Kath, O. Flores and H. A. Wilkinson, Non-invasive muscle contraction assay to study rodent models of sarcopenia, *BMC Musculoskeletal Disord.*, 2011, **12**, 246.
- 63 Y. H. Son, E. J. Jang, Y. W. Kim and J. H. Lee, Sulforaphane prevents dexamethasone-induced muscle atrophy via regulation of the Akt/Foxo1 axis in C2C12 myotubes, *Biomed. Pharmacother.*, 2017, **95**, 1486–1492.
- 64 Y. B. Chang, Y. Ahn, H. J. Suh and K. Jo, Yeast hydrolysate ameliorates dexamethasone-induced muscle atrophy by suppressing MuRF-1 expression in C2C12 cells and C57BL/6 mice, *J. Funct. Foods*, 2022, **90**, 104985, DOI: [10.1016/j.jff.2022.104985](https://doi.org/10.1016/j.jff.2022.104985).
- 65 D. Yaffe and O. Saxel, A myogenic cell line with altered serum requirements for differentiation, *Differentiation*, 1977, **7**, 159–166.
- 66 D. Yaffe and O. Saxel, Serial passaging and differentiation of myogenic cells isolated from dystrophic mouse muscle, *Nature*, 1977, **270**, 725–727.
- 67 J. V. Sharkey, Effect of acute low oxygen exposure on the proliferation rate, viability and myogenic regulatory gene expression of C2C12 myoblasts in vitro, *Arch. Stem Cell Ther.*, 2020, **1**, 1–9, DOI: [10.1101/2020.07.09.162123](https://doi.org/10.1101/2020.07.09.162123).
- 68 M. Sandri, J. Lin, C. Handschin, W. Yang, Z. P. Arany, S. H. Lecker, A. L. Goldberg and B. M. Spiegelman, PGC-1 α protects skeletal muscle from atrophy by suppressing FoxO3 action and atrophy-specific gene transcription, *Proc. Natl. Acad. Sci. U. S. A.*, 2006, **103**, 16260–16265.
- 69 L. Wang, X. F. Jiao, C. Wu, X. Q. Li, H. X. Sun, X. Y. Shen, K. Z. Zhang, C. Zhao, L. Liu, M. Wang, Y. L. Bu, J. W. Li, F. Xu, C. L. Chang, X. Lu and W. Gao, Trimetazidine attenuates dexamethasone-induced muscle atrophy via inhibiting NLRP3/GSDMD pathway-mediated pyroptosis, *Cell Death Discovery*, 2021, **7**, 251.
- 70 T. N. Stitt, D. Drujan, B. A. Clarke, F. Panaro, Y. Timofeyva, W. O. Kline, M. Gonzalez, G. D. Yancopoulos and D. J. Glass, The IGF-1/PI3K/Akt pathway prevents expression of muscle atrophy-induced ubiquitin ligases by inhibiting FOXO transcription factors, *Mol. Cell*, 2004, **14**, 395–403.
- 71 E. Seo, C. S. Truong and H. S. Jun, *Psoralea corylifolia* L. seed extract attenuates dexamethasone-induced muscle atrophy in mice by inhibition of oxidative stress and inflammation, *J. Ethnopharmacol.*, 2022, **296**, 115490.
- 72 S. Liu, D. Yang, L. Yu, Z. Aluo, Z. Zhang, Y. Qi, Y. Li, Z. Song, G. Xu and L. Zhou, Effects of lycopene on skeletal muscle-fiber type and high-fat diet-induced oxidative stress, *J. Nutr. Biochem.*, 2021, **87**, 108523.
- 73 R. J. Talmadge and R. R. Roy, Electrophoretic separation of rat skeletal muscle myosin heavy-chain isoforms, *J. Appl. Physiol.*, 1993, **75**, 2337–2340.
- 74 A. Fappi, J. C. Neves, L. N. Sanches, E. S. P. V. Massaroto, G. Y. Sikusawa, T. P. C. Brandao, G. Chadi and E. Zanoteli, Skeletal Muscle Response to Deflazacort, Dexamethasone and Methylprednisolone, *Cells*, 2019, **8**, 406.
- 75 T. Kohn and K. Myburgh, Regional specialization of rat quadriceps myosin heavy chain isoforms occurring in distal to proximal parts of middle and deep regions is not mirrored by citrate synthase activity, *J. Anat.*, 2007, **210**, 8–18.
- 76 S. Mueller, K. Saunier, C. Hanisch, E. Norin, L. Alm, T. Midtvedt, A. Cresci, S. Silvi, C. Orpianesi, M. C. Verdenelli, T. Clavel, C. Koebnick, H. J. Zunft, J. Dore and M. Blaut, Differences in fecal microbiota in different European study populations in relation to age, gender, and country: a cross-sectional study, *Appl. Environ. Microbiol.*, 2006, **72**, 1027–1033.
- 77 M. R. Charbonneau, L. V. Blanton, D. B. DiGiulio, D. A. Relman, C. B. Lebrilla, D. A. Mills and J. I. Gordon, A microbial perspective of human developmental biology, *Nature*, 2016, **535**, 48–55.
- 78 I. Sharon, M. J. Morowitz, B. C. Thomas, E. K. Costello, D. A. Relman and J. F. Banfield, Time series community genomics analysis reveals rapid shifts in bacterial species, strains, and phage during infant gut colonization, *Genome Res.*, 2013, **23**, 111–120.
- 79 B. Lakshminarayanan, C. Stanton, P. W. O'Toole and R. P. Ross, Compositional dynamics of the human intestinal microbiota with aging: implications for health, *J. Nutr., Health Aging*, 2014, **18**, 773–786.
- 80 F. Bifari, C. Ruocco, I. Decimo, G. Fumagalli, A. Valerio and E. Nisoli, Amino acid supplements and metabolic health: a potential interplay between intestinal microbiota and systems control, *Genes Nutr.*, 2017, **12**, 27.
- 81 P. W. O'Toole and I. B. Jeffery, Gut microbiota and aging, *Science*, 2015, **350**, 1214–1215.
- 82 A. M. Vaiserman, A. K. Koliada and F. Marotta, Gut microbiota: A player in aging and a target for anti-aging intervention, *Ageing Res. Rev.*, 2017, **35**, 36–45.
- 83 V. K. Ridaura, J. J. Faith, F. E. Rey, J. Cheng, A. E. Duncan, A. L. Kau, N. W. Griffin, V. Lombard, B. Henrissat, J. R. Bain, M. J. Muehlbauer, O. Ilkayeva, C. F. Semenkovich, K. Funai, D. K. Hayashi, B. J. Lyle, M. C. Martini, L. K. Ursell, J. C. Clemente, W. Van Treuren, W. A. Walters, R. Knight, C. B. Newgard, A. C. Heath and J. I. Gordon, Gut microbiota from twins discordant for obesity modulate metabolism in mice, *Science*, 2013, **341**, 1241214.
- 84 C. Chevalier, O. Stojanovic, D. J. Colin, N. Suarez-Zamorano, V. Tarallo, C. Veyrat-Durebex, D. Rigo,



- S. Fabbiano, A. Stevanovic, S. Hagemann, X. Montet, Y. Seimbille, N. Zamboni, S. Hapfelmeier and M. Trajkovski, Gut Microbiota Orchestrates Energy Homeostasis during Cold, *Cell*, 2015, **163**, 1360–1374.
- 85 G. H. van Muijlwijk, G. van Mierlo, P. W. Jansen, M. Vermeulen, N. M. Bleumink-Pluym, N. W. Palm, J. P. van Putten and M. R. de Zoete, Identification of Allobaculum mucolyticum as a novel human intestinal mucin degrader, *Gut Microbes*, 2021, **13**, 1966278.
- 86 X. Zhang, Y. Zhao, J. Xu, Z. Xue, M. Zhang, X. Pang, X. Zhang and L. Zhao, Modulation of gut microbiota by berberine and metformin during the treatment of high-fat diet-induced obesity in rats, *Sci. Rep.*, 2015, **5**, 14405.
- 87 S. Yang, D. Li, Z. Yu, Y. Li and M. Wu, Multi-Pharmacology of Berberine in Atherosclerosis and Metabolic Diseases: Potential Contribution of Gut Microbiota, *Front. Pharmacol.*, 2021, **12**, 709629.
- 88 Z. Yang, S. Huang, D. Zou, D. Dong, X. He, W. Liu and L. Huang, Metabolic shifts and structural changes in the gut microbiota upon branched-chain amino acid supplementation in middle-aged mice, *Amino Acids*, 2016, **48**, 2731–2745.
- 89 G. Corsetti, E. Pasini, G. D'Antona, E. Nisoli, V. Flati, D. Assanelli, F. S. Dioguardi and R. Bianchi, Morphometric changes induced by amino acid supplementation in skeletal and cardiac muscles of old mice, *Am. J. Cardiol.*, 2008, **101**, 26E–34E.
- 90 E. Nisoli, R. W. Grange and G. D'Antona, Nutrients and muscle disease, *BioMed Res. Int.*, 2015, **2015**, 809830.
- 91 D. Yamamoto, T. Maki, E. H. Herningtyas, N. Ikeshita, H. Shibahara, Y. Sugiyama, S. Nakanishi, K. Iida, G. Iguchi, Y. Takahashi, H. Kaji, K. Chihara and Y. Okimura, Branched-chain amino acids protect against dexamethasone-induced soleus muscle atrophy in rats, *Muscle Nerve*, 2010, **41**, 819–827.
- 92 Z. R. Xu, Z. J. Tan, Q. Zhang, Q. F. Gui and Y. M. Yang, The effectiveness of leucine on muscle protein synthesis, lean body mass and leg lean mass accretion in older people: a systematic review and meta-analysis, *Br. J. Nutr.*, 2015, **113**, 25–34.
- 93 E. Nisoli, V. Cozzi and M. O. Carruba, Amino acids and mitochondrial biogenesis, *Am. J. Cardiol.*, 2008, **101**, 22E–25E.
- 94 F. Bifari and E. Nisoli, Branched-chain amino acids differently modulate catabolic and anabolic states in mammals: a pharmacological point of view, *Br. J. Pharmacol.*, 2017, **174**, 1366–1377.
- 95 J. Angelin and M. Kavitha, Exopolysaccharides from probiotic bacteria and their health potential, *Int. J. Biol. Macromol.*, 2020, **162**, 853–865.
- 96 J. U. Kim, Y. Kim, K. S. Han, S. Oh, K. Y. Whang, J. N. Kim and S. H. Kim, Function of cell-bound and released exopolysaccharides produced by *Lactobacillus rhamnosus* ATCC 9595, *J. Microbiol. Biotechnol.*, 2006, **16**, 939–945.

